

---

# CatNet: Effective FDR Control in LSTM with Gaussian Mirrors and SHAP Feature Importance

---

**Jiaan Han, Junxiao Chen, Yanzhe Fu**

Department of Statistics, University of Michigan  
{jiaanhan, junxchen, yanzhefu}@umich.edu

## Abstract

We introduce CatNet, an algorithm that effectively controls False Discovery Rate (FDR) and selects significant features in LSTM with the Gaussian Mirror (GM) method. To evaluate the feature importance of LSTM in time series, we introduce a vector of the derivative of the SHapley Additive exPlanations (SHAP) to measure feature importance. We also propose a new kernel-based dependence measure to avoid multicollinearity in the GM algorithm, to make a robust feature selection with controlled FDR. We use simulated data to evaluate CatNet’s performance in both linear models and LSTM models with different link functions. The algorithm effectively controls the FDR while maintaining a high statistical power in all cases. We also evaluate the algorithm’s performance in different low-dimensional and high-dimensional cases, demonstrating its robustness in various input dimensions. To evaluate CatNet’s performance in real world applications, we construct a multi-factor investment portfolio to forecast the prices of S&P 500 index components. The results demonstrate that our model achieves superior predictive accuracy compared to traditional LSTM models without feature selection and FDR control. Additionally, CatNet effectively captures common market-driving features, which helps informed decision-making in financial markets by enhancing the interpretability of predictions. Our study integrates of the Gaussian Mirror algorithm with LSTM models for the first time, and introduces SHAP values as a new feature importance metric for FDR control methods, marking a significant advancement in feature selection and error control for neural networks.

## 1 Introduction

Deep Neural Networks have been widely proven as an accurate and generalizable method for prediction in many fields including image processing, biochemistry, and finance. However, as the DNN model become complex-structured, interpreting the model's prediction and underlying mechanism becomes extremely difficult. Model interpretation is important in many practical fields, since understanding the mechanism guides people to make rational real-world decisions. In such a setting, interpreting the influence of input features is essential for understanding the real significant factors. For example, in financial market predictions, we first need to discover the type of factors that make the largest contribution to the final result, and thus we can concentrate on analyzing these factors to make more rational and informed market predictions. It is also essential to extract the unimportant features in such a scenario, since these features may interact with other predictors and perplex the overall model, causing unexpected failures in the final prediction.

There are many previous works in measuring feature importance and selecting important features in neural networks. Hechtlinger [19] proposed a simple method to quantify feature importance by taking partial derivatives on each input feature. Verikas et al. [38] quantifies feature importance in Neural Networks by the changes in cross-validation error rate after removal of one feature. These methods are direct and rational, but fail to consider the inherent statistical errors of the model, which may cause unimportant features to have significant influences to final prediction. Such an error is a common phenomena which can be explained by a simple example in multiple linear regression: if a predictor  $x_j$  has no linear correlation with the label  $y$ , we may still falsely predict a coefficient  $\beta_j \neq 0$  with  $x_j$  due to multiple reasons. This is characterized as "False Discovery" or "Type I error" in statistical tests, and the expected value of the proportion of false discoveries relative to all discoveries (i.e. reject the null) is defined as the False Discovery Rate (FDR).

To construct a feature selection method which effectively controls the statistical errors, we need an effective approach to estimate and thus control the FDR. The method to control FDR was first proposed by Benjamini and Hochberg [5] by comparing p-values of multiple testing, which has been extensively studied and proven to be effective on linear models. However, in nonlinear models it is difficult to construct valid p-values for testing, since the distribution of the test statistics is usually unclear. Using Bootstrap or other methods to approximate p-values is valid but often impractical because of complex model and data structures or high computational costs.

To conquer such problems, Ke et al.[23] introduced a new generalized framework for effective FDR control algorithm, which can be summarized to three parts:

- (1) Construct an **importance metric** for each input feature and rank each feature by its importance
- (2) Create a **tampered design matrix** by adding fake variables.

(3) Calculate the feature importance of each fake variable in the design matrix which corresponds to each input feature, and convert the results into a **symmetric test statistic** which represents each input feature. The test statistic should be symmetric about zero for null variables ( $\beta_j = 0$ ) and take a large positive value for non-null variables ( $\beta_j \neq 0$ ). In other words, the input feature should be robust to perturbations added in the fake variables and remain significant under the test statistic to be considered a significant feature.

There are several methods that effectively controls the FDR under this framework. Barber et al. [2] introduced the "Knockoff Filter", which creates a "fake copy" of the feature matrix which maintains the original covariance structure but is independent of the responses. Comparing the inference results of the original features and the knockoff provides a valid selection of features while controlling the FDR. Candès et al. [8] proposed the Model-X Knockoff to extend this method to more complex models, and Lu et al. [26] used this model to control FDR in Deep Neural Networks. The Model-X Knockoff method is valid, but requires the distribution of inputs to be either exact or be within a distribution family that possesses simple sufficient statistics. Such assumption is not sufficient in many practical applications including medicine and finance. To propose a more general solution, Xing et al. [42] introduced the Gaussian Mirror algorithm, which measures the validity of each feature by adding a Gaussian noise to each input feature and analyzing its disturbance to the importance of each feature. The features are considered to be "Really Significant" if the change in its importance is smaller than a given threshold.

The Gaussian Mirror method is more reasonable and generalizable, but there still exist several problems. The first problem appears in the feature importance metric. The method they proposed to calculate feature importance is to track all weights in each neuron and sum over all path weights that connect the neurons. This method is a natural extension of the partial derivative method as proposed by Hechtlinger. These methods assume that we can approximate the contribution of the feature  $x_j$  to the output  $y$  by holding other variables constant and adding a small perturbation  $\Delta x_j$  to calculate the changes in output  $\Delta y$ . However, the assumption that "all other input features remain constant" is inappropriate because it assumes all other features are uncorrelated and orthogonal to  $x_j$  and thus do not change with  $x_j$ , which nearly impossible in real data.

To make such importance metric a practical and global measure, we introduce SHAP [28], which measures the input feature importance based on Shapley Values from game theory. It measures the influence of each feature to the output by computing the weighted average of the "Contribution Margin" of the feature to every possible combination of other features. This value accounts for the changes in all input variables and effectively considers their correlation. We take the derivative of the SHAP values of each feature as the measure of its importance, which can be interpreted as a "path derivative" which orients the direction  $x_j$  changes with other variables. This value provides a interpretable and global measure of the input feature importance, and is essentially useful in complex neural networks where the fitted function may differ significantly in different directions, such as CNN, LSTM, and

Transformers. In addition, we represent the importance of each feature  $x_j$  as a vector with each entry corresponding to each value of  $x_j$ , to quantify the change in the model's response to the feature following the change of feature values.

Another problem of the Neural Gaussian Mirror method appears in its construction of tampered design matrix. The construction of fake variables in this method aims to ensure that the distribution of these variables are uncorrelated, to avoid the instability of weight matrices in training due to multicollinearity, which will cause the feature importance measures to be very unstable and useless. To capture the possible non-linear correlations between variables which may lead to "Multicollinearity" in nonlinear models, Xing et al. proposed a kernel-based dependence metric, which maps the variables into high-dimensional space through kernel functions and capture its high-dimensional correlation. This method works well in MLP models, but it fails to consider the possible time-series correlation which may cause instability in training of time-series model or similar model that requires capturing the relationships between current and past observations, including models in the RNN-category (RNN, LSTM, etc.) and models with Attention mechanisms (Transformers, etc). To conquer such possible failure, we extend the Kernel-based Dependence Measure to consider the time-series cross-correlation of input features, to ensure the feature importance metric is robust in the training process.

In this paper, we introduce CatNet, an algorithm which modifies the Neural Gaussian Mirror method for FDR control in LSTM models for effective time-series prediction. We use SHAP values to measure feature importance and extended kernel method to construct the tampered design matrix. In addition, we use an extended version of the "signed max" of feature importance vector as a symmetric mirror statistic for effective FDR control. To test our algorithm's effectiveness and robustness, we experiment our algorithm with simulated data in both linear models and LSTM models. In linear models, we test CatNet's performance in both low-dimensional ( $p < n$ ) and high-dimensional ( $p > n$ ) cases and compare it with the original Gaussian Mirror method. The algorithm effectively controls the FDR under the preset level and maintains a very high statistical power. We then test CatNet's performance in different LSTM models by using different link functions demonstrating different nonlinear relations of the feature and the response. The algorithm still maintains a high power and controls the FDR under different dimensions and link functions. This displays that our algorithm is robust and generalizable in different time-series prediction models. To evaluate our algorithm's performance in real data, we construct a multi-factor portfolio for predicting the price of S&P 500 component stocks. We classify the factors into different categories and run the algorithm to select the significant factors. The simulation results demonstrate that the combined model with selected features make more accurate prediction compared to LSTM without feature selection and other common methods. Our method can detect abnormal macro-economic fluctuations and can generalize to other stocks not in our training set. We also conduct analysis of our selected factors to interpret the drivers of the stock market, showing that the method improves our understanding of the financial market and helps us make better informed future predictions.

**Our main contributions:**

- (1) To our knowledge, we are the first to extend the NGM algorithm in LSTM models. We take its main thoughts but change the construction of the feature importance metric, design matrix and mirror statistic to naturally extend it to more global cases, especially time-series models.
- (2) We are the first to use SHAP values to evaluate the feature importance in FDR control algorithms.
- (3) We are the first to introduce FDR Control in Neural Networks to stock market predictions. Previous works, such as [29], only use FDR control in linear models to make stock predictions and did not extend it to neural networks.

**2 Methods**

**2.1 LSTM**

Long Short-Term Memory (LSTM), first proposed by Hochreiter and Schmidhuber [20], is an advanced Recurrent Neural Network aiming to tackle the gradient vanishing or exploding problem in RNNs. It has been widely proven to be effective in time-series predictions, as its structure is designed to manage time-series memory.

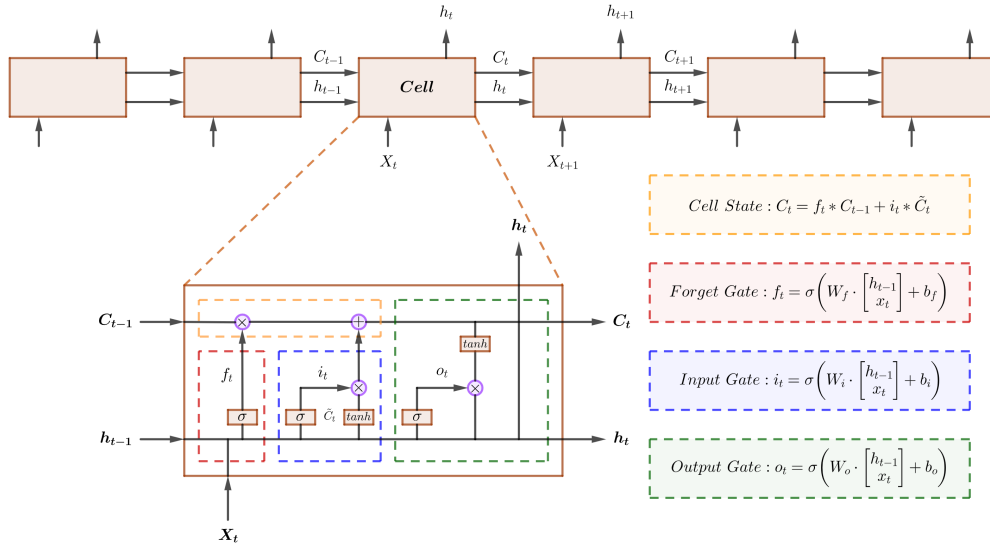


Figure 1: The structure of the LSTM

The key structure of LSTM is three gates: Input Gate, Output Gate and Forget Gate. For each element in the input sequence (time-series), LSTM computes the following:

$$\begin{aligned}
i_t &= \sigma(W_{ii}x_t + b_{ii} + W_{hi}h_{t-1} + b_{hi}) \\
f_t &= \sigma(W_{if}x_t + b_{if} + W_{hf}h_{t-1} + b_{hf}) \\
g_t &= \tanh(W_{ig}x_t + b_{ig} + W_{hg}h_{t-1} + b_{hg}) \\
o_t &= \sigma(W_{io}x_t + b_{io} + W_{ho}h_{t-1} + b_{ho}) \\
c_t &= f_t \odot c_{t-1} + i_t \odot g_t \\
h_t &= o_t \odot \tanh(c_t)
\end{aligned}$$

where  $h_t$  is the hidden state at time  $t$ ,  $c_t$  is the cell state at time  $t$ ,  $x_t$  is the input at time  $t$ ,  $h_{t-1}$  is the hidden state of the layer at time  $t - 1$  or the initial hidden state at time 0.  $i_t, f_t, g_t, o_t$  are the input, forget, cell, and output gates.  $\sigma$  is the sigmoid function, and  $\odot$  is the Hadamard product.

The memory cell  $c_t$  is the core of LSTM. It is the "memory" of previous input information stored in the model weights. The forget gate controls whether to retain or update the memory. The input gate controls whether to add current input into memory, and the output gate controls whether to add the output into hidden state. The output, or the predicted label of  $i$  at time  $t$  is denoted as:

$$\hat{y}_t^i = \text{Softmax}(h_t^i W_{fc}^i)$$

where  $W_{fc}$  is the matrix transforming the hidden state into the output.

LSTM has been widely used in time-series prediction tasks such as stock price predictions. In this paper, we construct the FDR control method which is designed for LSTMs but can also be generalized in more complex time-series prediction models.

## 2.2 Gaussian Mirror for FDR Control

Consider a linear regression model  $y = X\beta + \epsilon$  where  $\beta = \{\beta_1, \beta_2, \dots, \beta_p\}$  and  $X$  is the input matrix with  $n \times p$  dimensions. We want to test  $p$  hypotheses;  $H_j : \beta_j = 0$  for  $j = 1, \dots, p$  and find a rule to determine which hypotheses should be rejected. Let  $S_0 \subset \{1, 2, \dots, p\}$  be the set of predictors with  $\beta_j = 0$  and  $S_1$  be the set of effective predictors. We set  $\hat{S}_1$  be the set of selected effective predictors (i.e. reject the null hypothesis) by our statistical model. The FDR is defined as the expected value of the proportion of Type I error:

$$FDR = \mathbb{E}[FDP], \quad \text{where} \quad FDP = \frac{\#\{i \mid i \in S_0, i \in \hat{S}_1\}}{\#\{i \mid i \in \hat{S}_1\} \vee 1}.$$

Xing et al. [42] proposed the Gaussian Mirror method for controlling the FDR in linear regression models. For a given model  $y = X\beta + \epsilon$ , for each feature  $x_j$ , we construct

the mirror variables  $x_j^+ = x_j + c_j z_j$  and  $x_j^- = x_j - c_j z_j$ , where  $z_j \sim N(0, I_n)$  is an independently and identically distributed standard Gaussian random vector.

A key factor in constructing the Gaussian Mirror is to compute  $c_j$  to make the correlation of  $x_j^+$  and  $x_j^-$  closest to zero (given the other variables  $X_{-j}$ , which represents the feature matrix  $X$  subtracted by the the  $j$ -th column  $x_j$ ). If we did not set the correlation equal or close to zero,  $x_j^+$  and  $x_j^-$  will follow very similar distributions and their coefficients will be very unstable due to multi-collinearity. However, we hope that the regression coefficients of  $x_j^+$  and  $x_j^-$  are independent and thus can reflect the robustness of the original feature  $x_j$  subject to perturbations.

In a low-dimensional linear model ( $p < n$ ) and use ordinary least squares (OLS) for estimation, we can get an explicit expression of  $c_j$  to make the correlation equal to zero:

$$c_j = \sqrt{\frac{x_j^\top \left( I_n - X_{-j} (X_{-j}^\top X_{-j})^{-1} X_{-j}^\top \right) x_j}{z_j^\top \left( I_n - X_{-j} (X_{-j}^\top X_{-j})^{-1} X_{-j}^\top \right) z_j}}.$$

Then we construct the mirror statistic

$$M_j = \left| \hat{\beta}_j^+ + \hat{\beta}_j^- \right| - \left| \hat{\beta}_j^+ - \hat{\beta}_j^- \right|$$

We construct  $M_j$  so that, under the null hypothesis  $\beta_j = 0$ , by choosing the appropriate  $c_j$ , it is proven [42] that the distribution of  $M_j$  is symmetric about zero, that is,

$$\#\{j \in S_0 \mid M_j \geq t\} \approx \#\{j \in S_0 \mid M_j \leq -t\}$$

Based on this property, the false discovery proportion (FDP) can be estimated as

$$\widehat{\text{FDP}}(t) = \frac{\#\{j : M_j \leq -t\}}{\#\{j : M_j \geq t\} \vee 1},$$

In addition, [8] explained that the above formula is a slightly biased estimate of the FDP. For a more accurate estimate, we need to add the numerator by 1. Thus we estimate the FDP as

$$\widehat{\text{FDP}}(t) = \frac{\#\{j : M_j \leq -t\} + 1}{\#\{j : M_j \geq t\}},$$

and then a data-adaptive threshold

$$\tau_q = \min\{t > 0 : \widehat{\text{FDP}}(t) \leq q\}$$

is chosen to control the FDR at a preset level  $q$ .

The above method provides a basic framework of the Gaussian Mirror algorithm: (a) Add uncorrelated perturbation features for evaluating robustness, (b) Use a feature importance metric to rank features, (c) Construct the mirror statistic for feature selection. In later literature, we will examine each part and make proper improvements to extend it to general neural network models.

### 2.3 Feature Importance Vector for Mirror Statistic

We first start with the discussion for Part (c). In the previous literature, the feature importance metric, such as  $\beta_j$  in linear models, is represented by a scalar. It is under the assumption that the contribution of the  $j$ -th feature to the model outcome remains constant, and the specific values of the  $j$ -th feature do not alter its influence to the output. This assumption holds true for linear models, where the relationship between features and model output does not change relative to feature values. However, for more complex nonlinear models such as neural networks, the importance of a feature may vary depending on its input value, and a scalar value may no longer be sufficient to measure the global contribution of a feature. By such intuition, we introduce a vector-formed importance metric to accurately capture the change in feature importance through the input space.

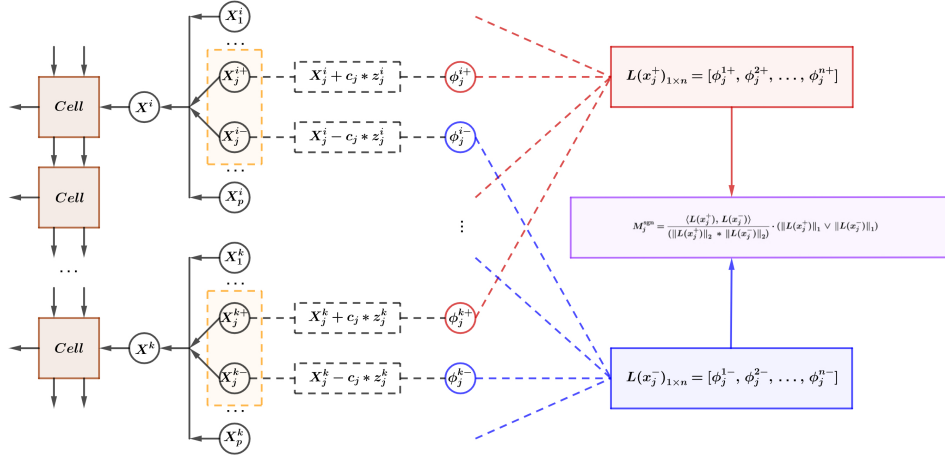


Figure 2: Flowchart of the  $j$ -th Mirror Statistic

For a training dataset with  $p$  features in an  $n$ -dimensional sample space  $X_{p \times n}$ , the feature importance can be represented as an  $p \times n$  matrix:

$$\phi_{p \times n} = \begin{pmatrix} \phi_1^1, \phi_1^2, \dots, \phi_1^n \\ \phi_2^1, \phi_2^2, \dots, \phi_2^n \\ \vdots \\ \phi_p^1, \phi_p^2, \dots, \phi_p^n \end{pmatrix}$$



where  $\phi_j^i$  measures the importance of the  $j$ -th feature when it takes the value of the  $i$ -th sample ( $x_{ji}$ ), and the  $j$ -th row of the matrix represents the importance vector of the  $j$ -th feature.

We compute the feature importance of the mirror variables  $x_j^+ = x_j + c_j z_j$  and  $x_j^- = x_j - c_j z_j$  by the same way. Now we have a training dataset with  $p + 1$  features in an  $n$ -dimensional sample space  $X'_{(p+1) \times n}$ , thus the feature importance is represented as:

$$\phi'_{(p+1) \times n} = \begin{pmatrix} \phi_1^1, \phi_1^2, \dots, \phi_1^n \\ \vdots \\ \phi_j^{1-}, \phi_j^{2-}, \dots, \phi_j^{n-} \\ \phi_j^{1+}, \phi_j^{2+}, \dots, \phi_j^{n+} \\ \vdots \\ \phi_p^1, \phi_p^2, \dots, \phi_p^n \end{pmatrix}$$

Then we construct the feature importance vector for the mirror variables:

$$L(x_j^-)_{1 \times n} = [\phi_j^{1-}, \phi_j^{2-}, \dots, \phi_j^{n-}], \quad L(x_j^+)_{1 \times n} = [\phi_j^{1+}, \phi_j^{2+}, \dots, \phi_j^{n+}]$$

Besides the mirror statistic Xing et al. [42] proposed before, Ke et al. [23] introduced another construction of the mirror statistic as the "signed-max":

$$M_j^{\text{sgn}} = \text{sgn}(\hat{\beta}_j^+ \cdot \hat{\beta}_j^-) \cdot (|\hat{\beta}_j^+| \vee |\hat{\beta}_j^-|)$$

where  $\hat{\beta}_j^+, \hat{\beta}_j^-$  are in scalar-form, and the statistic  $M_j^{\text{sgn}}$  for null features are symmetric around 0.

The first term in  $M_j^{\text{sgn}}$  needs to take a positive value when  $\hat{\beta}_j^+$  and  $\hat{\beta}_j^-$  share the same sign and a negative value when their signs differ. For two vectors, the Inner Product (dot product) can be used to effectively implement this function. Specifically, when two vectors orient the same direction in their space, the inner product is the largest possible positive number, indicating complete alignment. When the vectors are orthogonal, the inner product equals 0, reflecting no alignment. Conversely, when the vectors orient opposite directions in space, the inner product equals the smallest possible negative number, representing complete opposition. These values share the same meaning as the value and sign of corresponding scalar-valued functions.

Therefore, we consider using the Inner Product (Standardized by L2-norm) as a substitute for the sgn function:

$$\text{sgn}(\hat{\beta}_j^+ \cdot \hat{\beta}_j^-) \quad \longrightarrow \quad \frac{\langle L(x_j^+), L(x_j^-) \rangle}{(\|L(x_j^+)\|_2 * \|L(x_j^-)\|_2)}$$

The second term in  $M_j^{\text{sgn}}$  measures the maximum between the absolute value of  $\hat{\beta}_j^+$  and  $\hat{\beta}_j^-$ . To extend the expression to vector-form, we use the  $L_1$ -norm of the vector instead of the absolute value for scalar:

$$|\hat{\beta}_j^+| \vee |\hat{\beta}_j^-| \longrightarrow \|L(x_j^+)\|_1 \vee \|L(x_j^-)\|_1$$

where  $\|x\|_1 = \sum_{i=1}^n |x_i|$ .

So we can construct the mirror statistic for vector-form feature importance:

$$M_j^{\text{sgn}} = \frac{\langle L(x_j^+), L(x_j^-) \rangle}{(\|L(x_j^+)\|_2 * \|L(x_j^-)\|_2)} \cdot (\|L(x_j^+)\|_1 \vee \|L(x_j^-)\|_1)$$

## 2.4 SHAP Derivatives for Feature Importance

We now continue with Part (b). A common method to measure the contribution of the input features to the output is to take the partial derivative of the predicted output  $\hat{y}$  relative to the feature  $x_j$ :  $\phi_j = \frac{\partial \hat{y}}{\partial x_j}$ , as proposed by Hechtlinger [19]. Specifically for MLP models, Xing et al. [41] introduced a feature importance metric by tracking all paths that links the input feature to the output in the model and then summing over all path weights, which is a natural extension of the partial derivatives method. The problem that appears in both methods is that they assume that all variables are orthogonal to each other (i.e. completely uncorrelated), which is not true in nearly all real scenarios. Therefore, we need a measure that accounts for the change of other variables following the change on one input variable. In other words, we want to find the "path" that each input  $x_j$  moves in the feature space and take the derivative of the output on such a path. By this intuition, we come with SHAP values.

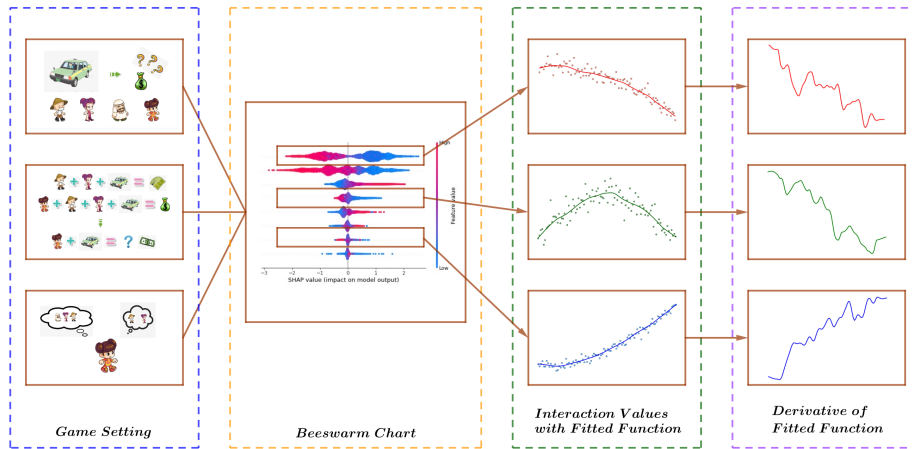


Figure 3: Flowchart of SHAP Feature Importance

### 2.4.1 SHAP Values

SHAP (SHapley Additive exPlanations), first introduced by Lundberg et al. [28] is a unified framework for interpreting machine learning model predictions by leveraging concepts from cooperative game theory. SHAP is rooted in the foundational work of Lloyd Shapley, who introduced the Shapley value in 1953 as a solution concept for the fair distribution of payoffs among players in a cooperative game. The Shapley value for a feature  $j$  is defined as:

$$\Phi_j = \sum_{S \subseteq N \setminus \{j\}} \frac{|S|! (|N| - |S| - 1)!}{|N|!} [v(S \cup \{j\}) - v(S)]$$

where  $N$  is the set of all features.  $S$  is a subset of features not containing  $j$ .  $v(S)$  is the value function representing the model's prediction using the feature subset  $S$ . The term  $\frac{|S|! (|N| - |S| - 1)!}{|N|!}$  serves as the weight factor for each coalition  $S$ .

SHAP extends the concept of Shapley values to machine learning by treating the prediction task as a cooperative game where each feature is a contributing player. Its value for each feature quantifies its contribution to the difference between the actual prediction and the average prediction. The SHAP value for a feature  $j$  is defined to be the same as its Shapley value, where the value function  $v(S)$  is given by:

$$v(S) = \mathbb{E}_{\mathbf{X} \setminus S} [f(\mathbf{x}_S \cup \mathbf{X} \setminus S)] - \mathbb{E}[f(\mathbf{X})]$$

Here,  $\mathbf{x}_S$  represents the feature values in subset  $S$  for instance  $i$ , and  $\mathbf{X} \setminus S$  denotes the random variables for the features not in  $S$ .

Formally, the value function is defined using integral:

$$v_{f, \mathbf{x}^{(i)}}(S) = \int f(\mathbf{x}_S^{(i)} \cup \mathbf{X}_C) dP(\mathbf{X}_C) - \mathbb{E}[f(\mathbf{X})]$$

For the coalition  $S$ , the feature values are set to those of the instance being explained, while the features not in  $S$  are treated as random variables sampled from their distribution  $P(\mathbf{X}_C)$ .

Substitute the value function  $v(S)$ , we get the expression for the SHAP value:

$$\Phi_j^i = \sum_{S \subseteq \{1, \dots, p\} \setminus \{j\}} \frac{|S|! (p - |S| - 1)!}{p!} \cdot (v(S \cup \{j\}) - v(S))$$

where the marginal contribution of feature  $j$  to coalition  $S$  is defined as:

$$v(S \cup \{j\}) - v(S) = \int f(\mathbf{x}_{S \cup \{j\}}^{(i)} \cup \mathbf{X}_{C \setminus \{j\}}) dP(\mathbf{X}_{C \setminus \{j\}}) - \int f(\mathbf{x}_S^{(i)} \cup \mathbf{X}_C) dP(\mathbf{X}_C)$$

Direct computation of SHAP values is computationally infeasible for models with a large number of features due to the exponential growth of feature coalitions. To address this, we use Monte Carlo sampling to estimate the SHAP values. We approximate the integral in the value function by sampling  $n$  background instances  $\mathbf{X}^{(k)}$ . The estimated value function for a coalition  $S$  is:

$$\hat{v}(S) = \frac{1}{n} \sum_{k=1}^n \left[ f \left( \mathbf{x}_S^{(i)} \cup \mathbf{X}_C^{(k)} \right) - f \left( \mathbf{X}^{(k)} \right) \right]$$

The marginal contribution of feature  $j$  to coalition  $S$  is then estimated as:

$$\Delta_{Sj} = \hat{v}(S \cup \{j\}) - \hat{v}(S) = \frac{1}{n} \sum_{k=1}^n \left[ f \left( \mathbf{x}_{S \cup \{j\}}^{(i)} \cup \mathbf{X}_{C \setminus \{j\}}^{(k)} \right) - f \left( \mathbf{x}_S^{(i)} \cup \mathbf{X}_C^{(k)} \right) \right]$$

After traversing all possible coalitions, the estimated SHAP value for feature  $j$  is:

$$\hat{\Phi}_j^i = \sum_{S \subseteq \{1, \dots, p\} \setminus \{j\}} \frac{|S|! (p - |S| - 1)!}{p!} \Delta_{Sj}$$

SHAP values satisfy several desirable properties that ensure fair and consistent attribution of feature importance. Based on these properties, we can construct our feature importance metric based on SHAP values. (See Appendix A for details).

#### 2.4.2 Feature Importance Metric Based on SHAP

Based on Lemma 1 (See Appendix A), we know that the summation of SHAP values  $\Phi_j$  of all features  $j$  equals the difference between the predicted value of  $y$  and the expected value of model prediction. We can treat this expected value as a constant since it does not change with the value of the features.

$$\sum_{j=1}^p \Phi_j = \hat{f}(x) - \mathbb{E}_X[\hat{f}(X)] = \hat{y} + C$$

Therefore, we can treat the SHAP values as "dividing" the output  $\hat{y}$  into parts  $\hat{y} = \Phi_1 + \dots + \Phi_p$  for  $p$  input features, each function  $\Phi_j(x_1, \dots, x_j, \dots, x_p)$  represents the SHAP value of feature  $j$  relative to all features since calculating its value requires considering all possible coalitions of  $(x_1, \dots, x_{j-1}, x_{j+1}, \dots, x_p)$ . The derivative  $\frac{\partial \Phi_j}{\partial x_j}$ , in contrast to previous methods that directly calculates  $\frac{\partial \hat{y}}{\partial x_j}$ , takes into account the weighted average of movements of other input variables, which estimates the movements of other variables with minor change  $\Delta x_j$  in the  $j$ -th feature due to their correlation. Therefore, we can use the partial derivative of the SHAP value relative to the input feature as a more reliable importance metric:

$$\phi_j^t = \frac{\partial \Phi_j^t}{\partial x_j}$$

It can be easily proved that in linear regression models, the expected value of  $\phi_j$  across all  $t$  equals the regression coefficient  $\beta_j$  (See Appendix B). So this measure is also a natural extension of regression coefficients.

In real scenarios, the SHAP values  $\Phi_j$  of  $x_j$  in all times  $t$  will be noised due to the intrinsic random noise in  $x_j$ . So we need to use a smooth function to fit the scatterplot of  $\Phi_j$  relative to  $x_j$  and take the slope of the fitted function in each input value  $x_j^t$ , to minimize the impact of random noises. In practice, we find Lowess smoothing sufficient for fitting this function and get the desired result.

Then we can construct the feature importance vector and the mirror statistic as noted before:

$$L(x_j^-)_{1 \times n} = [\phi_j^{1-}, \phi_j^{2-}, \dots, \phi_j^{n-}], \quad L(x_j^+)_{1 \times n} = [\phi_j^{1+}, \phi_j^{2+}, \dots, \phi_j^{n+}]$$

$$M_j^{\text{sgn}} = \frac{\langle L(x_j^+), L(x_j^-) \rangle}{(\|L(x_j^+)\|_2 * \|L(x_j^-)\|_2)} \cdot (\|L(x_j^+)\|_1 \vee \|L(x_j^-)\|_1)$$

For a null feature  $j$ , the expectation of the SHAP value in all values of  $x_j$  is zero (See Property 2 in Appendix A). So the derivatives of the smoothed function SHAP values should be a small value randomly distributed around zero, and the mirror statistic should be equally distributed around zero. For non-null features, the absolute value of the derivatives should be large and the corresponding mirror statistic will take a large positive value. This fulfills the requirement for the mirror statistic in the Gaussian Mirror algorithm for an effective FDR control.

## 2.5 Kernel-Based Dependence Measure

In this part, we consider the construction of the mirror variables  $x_j^+$  and  $x_j^-$  in Part (a). The reason that we need the distribution of these two variables uncorrelated can be simply explained by a linear regression example. Consider a simple linear regression model  $y = \beta_0 x_0 + \epsilon$ . If we take two variables  $x_1$  and  $x_2$  to be exactly from the same distribution as  $x_0$  and regress  $y$  on these two variables:  $y = \beta_1 x_1 + \beta_2 x_2 + \epsilon$ , then theoretically  $\beta_1 + \beta_2 = \beta_0$ , and  $\beta_1, \beta_2$  can take any value that sum to  $\beta_0$  since they are totally correlated. In other words, high multicollinearity of the two variables causes the regression coefficients to be highly correlated and unstable. In the Gaussian Mirror algorithm, if we make  $x_j^+$  and  $x_j^-$  highly correlated, the weights of the fitted model will be highly unstable and may be totally different. Since we want to test the robustness of the input feature in one stable model, we need to avoid the model's intrinsic instability due to such multicollinearity issues.

In linear models, we can simply minimize the Pearson correlation coefficient of  $x_j^+$  and  $x_j^-$ . However, non-linear models may capture the non-linear correlations between the variables

which the Pearson correlation coefficient cannot quantify. For example, if two variables  $x_1$  and  $x_2$  has  $x_2 = \sin(x_1)$ , their Pearson correlation coefficient may be very small, but Neural Networks are highly likely to capture such a correlation, causing highly unstable gradients in back-propagation and thus unstable weight matrices in the model. As a result, we need a dependence measure that can effectively capture the non-linear correlation between two variables.

A natural thought is to map the feature values into high-dimensional space through a kernel function to capture the high-dimensional correlation, which corresponds to the non-linear correlations in the original feature space. Gretton et al. [17] proposed the Hilbert-Schmidt Independence Criterion (HSIC) which effectively quantifies this kernel-based independence measure:

$$\text{HSIC}(X, Y) = \|C_{XY}\|_{\text{HS}}^2$$

where  $C_{XY}$  is the covariance operator of  $X$  and  $Y$  in the Reduced Kernel Hilbert Space (RKHS) that the kernel function maps to, and  $\|\cdot\|_{\text{HS}}$  is the Hilbert-Schmidt norm.

For a sample  $\{(x_i, y_i)\}_{i=1}^n$ , the unbiased estimator of HSIC is:

$$\text{HSIC}_n = \frac{1}{(n-1)^2} \text{tr}(\tilde{K}\tilde{L}) \quad \tilde{K} = HKH, \tilde{L} = HLH$$

where  $K, L$  are the kernel matrices  $K_{ij} = k(x_i, x_j)$ ,  $L_{ij} = l(y_i, y_j)$ ,  $H$  is the centering matrix  $H = I - \frac{1}{n}11^T$  to standardize the kernel matrices and  $\text{tr}$  is the trace of the matrix.

For linear kernels, we can prove that HSIC is proportional to the square of Pearson correlation coefficient (See Appendix C). For non-linear kernels, HSIC can be viewed as extending the Pearson Correlation Coefficient into high-dimensional feature space to capture correlations unobserved in low-dimensional space.

In the Gaussian Mirror method, we need the mirror variables  $x_j^+$  and  $x_j^-$  to be independent conditional on  $x_{-j}$ . To measure the conditional independence and save computational costs, Xing et al. [41] transformed the calculation of HSIC in Gaussian Mirrors to the following equivalent form:

$$\text{HSIC} = \frac{1}{n^2} [(HK^U H) \circ (HK^V H) \circ K^W]_{++}$$

where  $[A]_{++} = \sum_{i=1}^n \sum_{j=1}^n A_{ij}$  and  $\circ$  is the Hadamard product.  $K^U, K^V, K^W$  are the kernel matrices for  $x_j^+, x_j^-, x_{-j}$ , respectively. The denominator  $n^2$  and  $(n-1)^2$  does not matter since we only need to find the minimum of HSIC in this case. This approach has an approximately  $O(n)$  complexity with parallel computing compared to the  $O(n^2)$  complexity of the original formula for HSIC.

However, to extend the Gaussian Mirror algorithm into time-series models, such an HSIC value is not sufficient. The main problem is that this measure only considers the correlation between  $x_1^t$  and  $x_2^t$  for two variables  $x_1, x_2$ , but fails to capture their time-series cross-correlation. Avoiding such cross-correlation is essential in time-series models. Take a simple example in LSTM, if we set the look-back time of LSTM to be 60, then the model will calculate the weights that the past 60 inputs contribute to the current input. In this case, if we set  $x_2^t = x_1^{t+1}$ , then suppose the weight matrices for all look-back times are:

$$W_1 = (w_1^{t-60}, w_1^{t-59}, \dots, w_1^{t-2}, w_1^{t-1}) = (0, 0, \dots, 0, 1)$$

$$W_2 = (w_2^{t-60}, w_2^{t-59}, \dots, w_2^{t-2}, w_2^{t-1}) = (0, 0, \dots, 1, 0)$$

Then  $W_1$  and  $W_2$  contributes the same to the model output. And training this model a second time may lead to completely different weights in  $W_1$  and  $W_2$ , similar to the multicollinearity issue in linear regression. To capture this correlation, we need to compute the HSIC value for a time-lapse  $\tau$ :

$$\text{HSIC}_\tau(X, Y) = \frac{1}{(n-1)^2} \text{tr}(\tilde{K}^t \tilde{L}^{t-\tau})$$

where  $K_{ij} = k(x_i^t, x_j^t)$ ,  $L_{ij} = k(y_i^{t-\tau}, y_j^{t-\tau})$ .

LSTM considers the feature value of  $k$  lookback times, so we need to consider the HSIC value for all  $\tau = \{1, \dots, k\}$ . We take the weighted sum of all HSIC values as the final Dependence Measure:

$$I = \sum_{\tau=0}^k w_\tau \text{HSIC}_\tau(X, Y) = \sum_{\tau=0}^k w_\tau \frac{1}{(n-1)^2} \text{tr}(\tilde{K}^t \tilde{L}^{t-\tau})$$

where  $\sum_{\tau=0}^k w_\tau = 1$ . The value with  $\tau = 0$  represents the normal non-time-series correlation between X and Y. We take the weighted sum because LSTM tends to consider values closer to current time over earlier values, so the correlation with earlier values are not so important. We can take the empirical formula  $w_\tau = a \cdot \exp(-\frac{1}{10}\tau)$ , where  $a$  is the factor that scales the sum to 1.

Then we can transform this measure into the conditional dependence measure required for constructing the mirror variables in the Gaussian Mirror algorithm:

$$I_j(c) = \sum_{\tau=0}^k w_\tau \text{HSIC}_\tau(X, Y) = \frac{1}{n^2} \sum_{\tau=0}^k w_\tau [(HK_t^U H) \circ (HK_{t-\tau}^V H) \circ K^W]_{++}$$

And then we take  $c_j$  to be the the argmin of the dependence measure:

$$c_j = \arg \min_c I_j(c)$$

to construct the mirror variables  $x_j^+ = x_j + c_j z_j$  and  $x_j^- = x_j - c_j z_j$ .

In practice, we compute the optimal  $c_j$  by taking a uniform range of values of  $c$  within a relatively large interval, and calculate the corresponding values of  $I_j$  to fit the function. Then we subtract the range where the minimum value of  $I_j(c)$  approximately exists, and use Cubic Spline Interpolation to fit the function of  $I_j(c)$  within this range and find the minimum. We find that  $I_j(c)$  is always a convex smooth function, allowing us to use interpolation to approximate the value of  $c_j$  within the error bound of the fourth derivative of  $I_j(c)$ .

## 2.6 CatNet

Now we can summarize our CatNet algorithm, which efficiently selects the significant features in the LSTM model and controls the FDR under the preset level:

---

### Algorithm 1 CatNet - Effective Feature Selection in LSTM

---

**Input:** Fixed FDR level  $q$ ,  $(x_i, y_i)$ ,  $i = 1, \dots, n$  with  $x_i \in \mathbb{R}^p$ ,  $y_i \in \mathbb{R}^1$

**Output:**  $\hat{S}_1$

1. **for**  $i = 1$  to  $p$ , **do**:

A. Generate  $Z_j \sim \mathcal{N}(0, I_n)$ .

B. Calculate  $c_j = \arg \min_c I_j = \arg \min_c \sum_{\tau=0}^k w_\tau \text{HSIC}_\tau(X, Y)$ .

C. Construct mirrored pair  $(X_j^+, X_j^-) = (X_j + c_j Z_j, X_j - c_j Z_j)$ .

D. Train LSTM with  $X^{(j)} = (X_j^+, X_j^-, X_{-j})$  as the input data.

E. Compute the SHAP values for  $X_j^+, X_j^-$

F. Take the derivatives of SHAP values  $L(x_j^-) = [\phi_j^{1-}, \phi_j^{2-}, \dots, \phi_j^{n-}]$ ,  
 $L(x_j^+) = [\phi_j^{1+}, \phi_j^{2+}, \dots, \phi_j^{n+}]$  as the feature importance vector

G. Compute statistic  $M_j = \frac{\langle L(x_j^+), L(x_j^-) \rangle}{(\|L(x_j^+)\|_2 * \|L(x_j^-)\|_2)} \cdot (\|L(x_j^+)\|_1 \vee \|L(x_j^-)\|_1)$ .

**end for**

2. Calculate  $T = \min\{t > 0 : \text{FDP}(t) \leq q\}$ .

3. Return  $\hat{S}_1 \leftarrow \{j : M_j \geq T\}$ .

---

Though this algorithm is designed for LSTM model, we suppose it can be easily extended to other time-series prediction models such as RNN and GRU. It may also be generalized to Attention models with minor changes, since they both emphasizes the relation of past observations with current observation.

To increase computational efficiency, we also construct an algorithm which construct the mirror variable of the  $p$  input features at the same time. Denoted as Simultaneous-CatNet (S-CatNet). In later simulations, we demonstrate that S-CatNet also effectively controls the FDR and maintains a high power.



---

**Algorithm 2** S-CatNet - Simultaneous Feature Selection in LSTM

---

**Input:** Fixed FDR level  $q$ ,  $(x_i, y_i)$ ,  $i = 1, \dots, n$  with  $x_i \in \mathbb{R}^p$ ,  $y_i \in \mathbb{R}^1$

**Output:**  $\hat{S}_1$

1. **for**  $i = 1$  to  $p$ , **do**:
    - A. Generate  $Z_j \sim \mathcal{N}(0, I_n)$ .
    - B. Calculate  $c_j = \arg \min_c I_j = \arg \min_c \sum_{\tau=0}^k w_\tau \text{HSIC}_\tau(X, Y)$ .
    - C. Construct mirrored pair  $(X_j^+, X_j^-) = (X_j + c_j Z_j, X_j - c_j Z_j)$ .
  - end for**
  2. Train LSTM with  $X = (X_1^+, X_1^-, \dots, X_p^+, X_p^-)$  as the input data.
  3. Compute the SHAP values for  $X_1^+, X_1^-, \dots, X_p^+, X_p^-$
  4. Take the derivatives of SHAP values  $L(x_j^-) = [\phi_j^{1-}, \phi_j^{2-}, \dots, \phi_j^{n-}]$ ,  
 $L(x_j^+) = [\phi_j^{1+}, \phi_j^{2+}, \dots, \phi_j^{n+}]$  as the feature importance vector
  5. Compute mirror statistics  $M_j = \frac{\langle L(x_j^+), L(x_j^-) \rangle}{(\|L(x_j^+)\|_2 * \|L(x_j^-)\|_2)} \cdot (\|L(x_j^+)\|_1 \vee \|L(x_j^-)\|_1)$ .
  6. Calculate threshold  $T = \min\{t > 0 : \hat{\text{FDP}}(t) \leq q\}$ .
  7. Return  $\hat{S}_1 \leftarrow \{j : M_j \geq T\}$ .
- 

### 3 Numerical Simulations

To evaluate the effectiveness and robustness of CatNet, we consider its effect in both Linear Model and LSTM.

#### 3.1 Linear Models

For linear models, we generate all input variables  $X$  from a standard Gaussian distribution  $\mathcal{N}(0, 1)$ . We assume the input variables  $X$  and the response  $y$  follow a linear model:  $y_i = \beta^T x_i + \epsilon_i$ ,  $\epsilon_i \stackrel{\text{i.i.d.}}{\sim} \mathcal{N}(0, 1)$ . We randomly set  $k$  elements in  $\beta$  to be nonzero and generate  $\beta$  from  $\mathcal{N}\left(0, \left(20\sqrt{\log(p)/n}\right)^2\right)$ . The  $k$  variables with nonzero  $\beta$  values are considered to be relevant features. By running our algorithm, we want to select the relevant features we set and reject all other features as null features since they can be seen as random noises.

We run the CatNet algorithm in different numbers of input features  $p$  and data length  $n$ . For the low-dimensional cases where  $p < n$ , we keep the proportion of relevant features and null features to be 1 : 4. For high-dimensional cases where  $p \geq n$ , we keep the proportion of relevant features and the data length  $n$  to be 1 : 10 to mimic the sparsity of significant features in high-dimensional regression. In cases where  $p \geq n$ , we first use LASSO to select the features as part of our algorithm, and then run the simple linear regression to construct the mirror statistic. We set the FDR level  $q = 0.1$  and test the FDR and Power of our algorithm in  $p = 125 \sim 1500$  and  $n = 250 \sim 3000$ . For each test, we repeat 30 times and take the mean value.

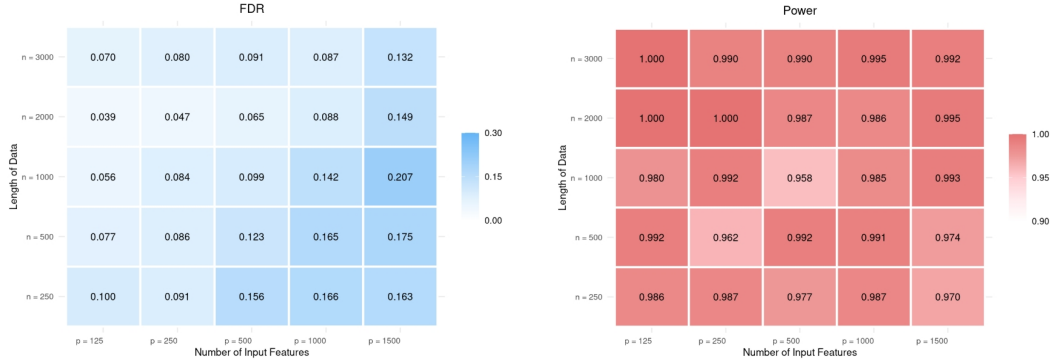


Figure 4: FDR and Power on Linear Model using the CatNet algorithm

As shown in Figure 4, we found that CatNet maintains a very high power (close to 1) in all values of  $p$  and  $n$  and effectively controls the FDR under the preset level when  $p < n$ . In high dimensional cases where  $p \geq n$ , we sometimes fail to control the FDR under the given level. However, this is not due to the inefficiency of our algorithm. The reason is that LASSO causes the distribution of the mirror statistic for null features to be left-skewed instead of symmetric. Using the Debiased LASSO [44] can effectively minimize such problem and control the FDR under the given level.

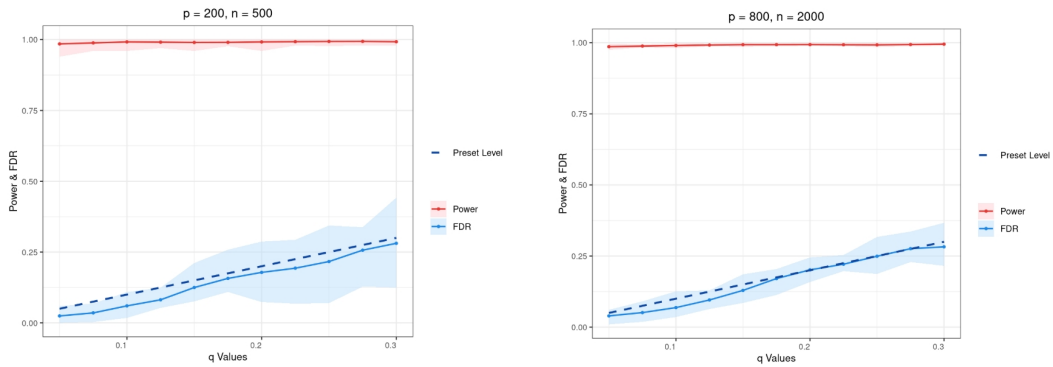


Figure 5: FDR and Power on Linear Models for  $p = 200, n = 500$  and  $p = 800, n = 2000$

To evaluate CatNet’s Performance under different preset level  $q$ , we consider two cases:  $p = 200, n = 500$  and  $p = 800, n = 2000$  and take different values of  $q$  between 0.05 and 0.30. As shown in Figure 5, we found that in both cases, smaller  $q$  ( $q < 0.2$ ) more effectively controls the FDR. Setting  $q$  too high causes the FDR level to be unstable, partly because the cutoff value for mirror will be chosen in the range of the null variables, which make unexpected large numbers of null variables included in the selected features.

We also test CatNet’s performance in different settings of correlation within the relevant input features, to test its robustness in highly correlated features. We control the relative correlation within the relevant features by generating a covariance matrix  $\Sigma$  and use Cholesky

Decomposition to decompose the covariance matrix and add correlation to each feature. In addition, we compare the results with the original Gaussian Mirror algorithm in both low-dimensional ( $p = 500, n = 1000$ ) and high-dimensional ( $p = 1000, n = 500$ ) cases. Our experiment shows that the power of CatNet remains similar to the original GM algorithm in all cases, and the FDR is slightly lower. This demonstrates that our method can be generalized as a natural extension of the Gaussian Mirror method in linear cases.

Setting ( $p, n$ )	Correlation Coef.	CatNet		GM	
		FDR	Power	FDR	Power
$p = 500, n = 1000$	0.2	0.076	0.949	0.146	0.925
	0.5	0.078	0.946	0.122	0.899
	0.8	0.047	0.895	0.118	0.929
$p = 1000, n = 500$	0.2	0.121	0.889	0.151	0.963
	0.4	0.116	0.812	0.143	0.819
	0.6	0.124	0.701	0.122	0.659

Table 1: Performance of CatNet and GM in different correlation coefficients

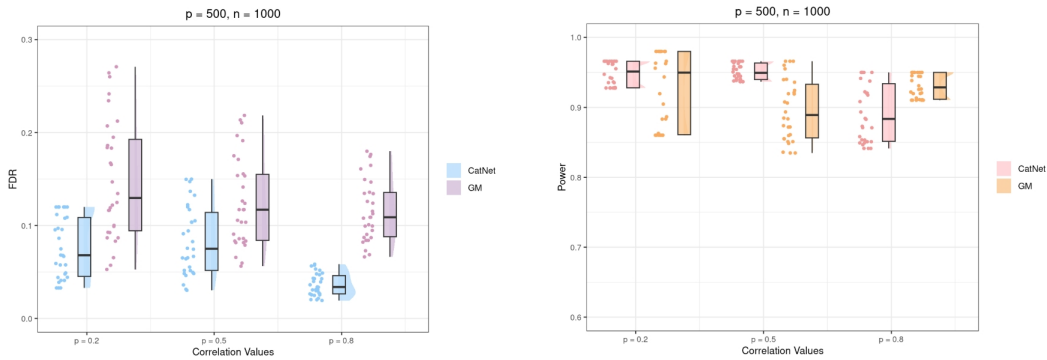


Figure 6: FDR and Power on Linear Models for  $p = 500, n = 1000$ .

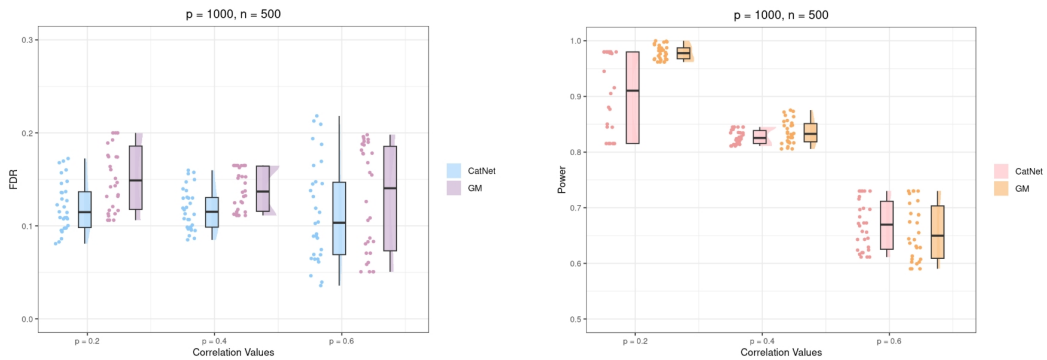


Figure 7: FDR and Power on Linear Models for  $p = 1000, n = 500$ .

### 3.2 LSTM Models

We further test the performance of CatNet in different settings of LSTM models. To simulate time-series data for LSTM training, we need to generate features with high time-series autocorrelation and relatively low correlations across features. By this intuition, we use the Brownian Motion to simulate the time-series data. We assume the starting value  $x_0$  of each motion to be a random value from  $\mathcal{N}(0, 1)$ , and for each later time step  $t$ , we take  $x_t$  from  $\mathcal{N}(x_{t-1}, 1)$ . For null features, we just take a random value from  $\mathcal{N}(0, 1)$  for all time steps. This simulated data from Brownian Motion ensures that each feature has high time-series autocorrelation, and they are all independent and identically distributed.

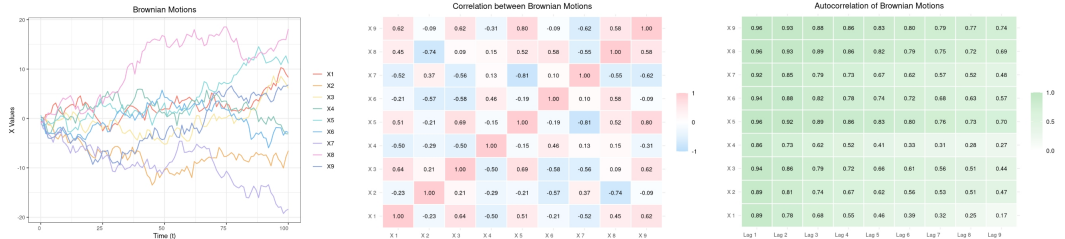


Figure 8: Brownian Motions for LSTM simulation. Left: Time-Series plot of 9 randomly generated Brownian Motions. Middle: Correlation matrix of the 9 motions. Right: Time-Series autocorrelation of the 9 motions

Then we generate  $z_i = \beta^T x_i + \epsilon_i, \epsilon_i \stackrel{\text{i.i.d.}}{\sim} \mathcal{N}(0, 1)$  with the same method to choose  $\beta$  as in linear models. To mimic the different types of relation of the response  $y$  with the input  $X$ , we add a link function  $y(z)$  to the temporary value  $z$  to generate the final response vector  $y$ . We consider three link functions:  $y(z) = z$ ,  $y(z) = \sin(z/a) \cdot \exp((x + b)/c)$  and  $y(z) = a \cdot \arcsin(\sin(z/b))$ . We choose an LSTM with two hidden layers with hidden layer dimension  $N = 20 \log(p)$ . We experiment on both high-dimensional cases where  $p = 1000, n = 500$  and low-dimensional cases where  $p = 500, n = 1000$ . We also experiment on our CatNet algorithm with our improved Time-Series Kernel Dependence and the original Kernel Dependence that does not account for time-series correlations, to test whether our metric effectively mitigates the time-series multicollinearity. For each test, we repeat 30 times and plot the confidence interval for the FDR and Power. To save computational time, we use the S-CatNet algorithm, which in practice does not show significant loss in performance compared to the original CatNet.

Setting ( $p, n$ )	Link function	TS Kernel		Non-TS Kernel	
		FDR	Power	FDR	Power
$p = 500, n = 1000$	$t$	0.097	0.854	0.189	0.797
	$\sin(t/100) \exp(t/500 + 2)$	0.060	0.873	0.094	0.843
	$10 \arcsin(\sin(t/100))$	0.059	0.919	0.071	0.894
$p = 1000, n = 500$	$t$	0.033	0.732	0.047	0.665
	$\sin(t/100) \exp(t/500 + 2)$	0.079	0.925	0.097	0.901
	$10 \arcsin(\sin(t/100))$	0.101	0.876	0.122	0.839

Table 2: Performance of CatNet in different link functions with two Kernel Dependence

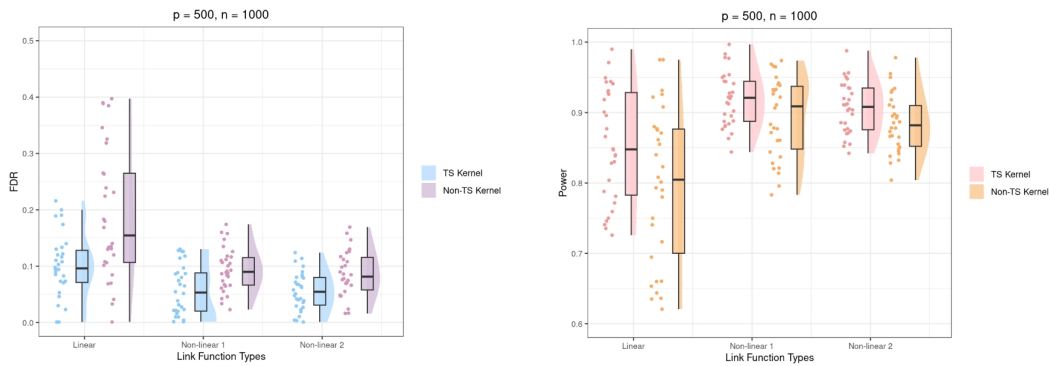


Figure 9: FDR and Power on LSTM for  $p = 500, n = 1000$  with different Kernel Dependence

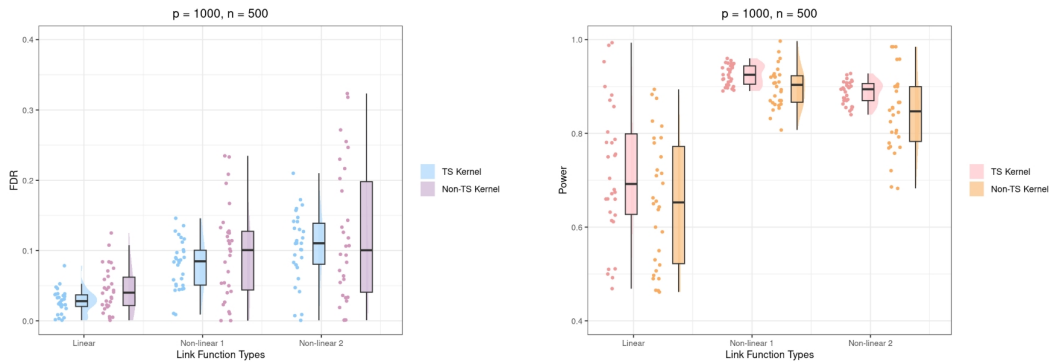


Figure 10: FDR and Power on LSTM for  $p = 1000, n = 500$  with different Kernel Dependence

We found that given the preset level  $q = 0.2$ , CatNet effectively controls the FDR and maintains a power larger than 0.9 for the two nonlinear link functions in both the high-dimensional and the low-dimensional case. For the linear link function, CatNet still effectively controls the FDR, but the power is relatively low, partly due to possible overfitting of the LSTM model. In addition, the time-series kernel does not clearly improve the mean value of FDR and power, but it clearly reduces the variance, making our algorithm more robust. In a

few cases where a significant time-series relation exist, the original kernel fail to minimize this relation and multicollinearity issues still exist. This causes the mirror statistic or some relevant features to become a large negative value, which fails the algorithm. In contrast, our kernel dependence mitigates this multicollinearity issue in time-series and mitigates the failure of the algorithm.

#### 4 Application in Real World Stock Data

To evaluate CatNet’s performance in real-world applications, we construct a multi-factor portfolio for predicting the stock prices of S&P 500 components. We compare the LSTM model with the original input data and the input data after CatNet’s selection to evaluate its improvement in prediction accuracy and generalization in interpreting market factors.

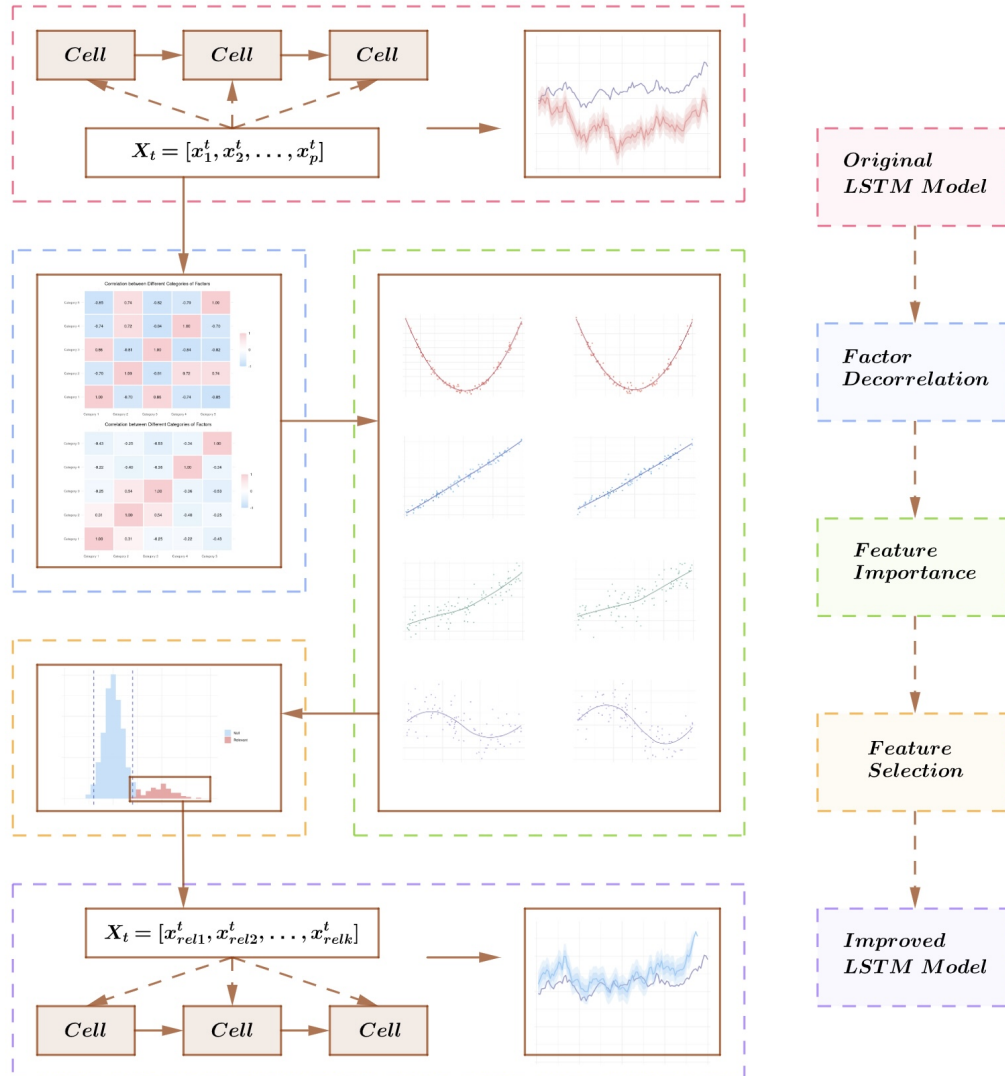


Figure 11: Flowchart of our model in Stock Prediction

## 4.1 Data Collection and Pre-processing

Our data consists of historical daily-frequency data of S&P 500 Index component stocks and of macroeconomic indicators, all ranging from 01/01/2006 to 09/30/2024. The data source are mainly Yahoo Finance and Wind financial terminal. There are mainly three categories:

(1) Historical trading information of S&P 500 Components. These include price fluctuations, trading volume, turnover rate, fraction of large and small orders, etc. These are firm-specific numerical data representing the trading activity of the stock market.

(2) Financial Reports and Valuation metrics of S&P 500 Components. These include balance sheets, cash flow reports, income reports, and common valuation metrics such as P/E and P/B ratio. They are the basic fundamental analysis metrics commonly used in financial analysis, reflecting the operating performance and growth potentials of a company which affects its future stock price.

(3) Macroeconomic factors including GDP, CPI, Interest Rates, Exchange Rates, Special Events, etc. These data are not firm-specific and reflects the overall macroeconomic environment which may shape the whole financial market. Such factors are extremely important in identifying some abnormal fluctuations of the market due to special events, for example, the COVID-19 pandemic in 2020.

We collect the data for each stock and combine them with the macroeconomic indicators to construct the training data for predicting each stock. Each feature represents one factor that possibly influence the stock price fluctuations.

## 4.2 Factor Classification, Dimension Reduction and De-correlation

### 4.2.1 Factor Categories

To construct a multi-factor stock prediction model and evaluate its utility in interpreting the financial market, we categorize each factor according to their financial attributes and the roles they play in explaining price fluctuations. We categorize the factors into five main categories:

**Market Price Factors:** These factors represent trading metrics that directly reflect the market performance of individual stocks, including the Open Price, Close Price, High / Low Price, Trading Volumes, etc.

**Fundamental Financial Factors:** These factors capture company-level performance metrics and financial health indicators derived from each company's financial reports. Typical factors include Net Income, Cash Flows, PE Ratio, etc.

**Macroeconomic Factors:** These factors capture broader economic trends and policy-related variables that influence the financial market, including GDP Growth of different countries, CPI, Unemployment Rate, Money Supply, Trade Balance, etc.

**Industry-Specific Factors:** These factors reflect industry-specific trends and sectoral dynamics, including PPIs of important industries such as Real Estate, Telecommunication, Transportation, etc.

**Momentum Factors:** These factors measure patterns and trends in stock price movements, often reflecting behavioral finance principles. They include short-term and long-term metrics such as mean, standard deviation, skewness, and kurtosis of returns.

#### 4.2.2 Dimension Reduction and De-correlation

To address potential multi-collinearity and redundant information, we apply a systematic dimension reduction and de-correlation process across the categorized factors. This process ensures that the resulting factors are interpretable, minimally correlated, and retain the majority of their explanatory power.

We first perform intra-category correlation analysis. We use Variance Inflation Factor (VIF) analysis within each category to evaluate multicollinearity among factors. Factors with  $VIF \leq 5$  are retained directly as they exhibit low multicollinearity.

For the highly collinear factors ( $VIF > 5$ ), we take each factor  $x_i$  as the response variable and other factors  $x_1, \dots, x_{i-1}, x_{i+1}, \dots, x_p$  as the predictors and take the residual as the new factor value for  $x_i$ .

$$x_i = \beta_1 x_1 + \beta_2 x_2 + \dots + \beta_p x_p + \epsilon_i,$$

This ensures that  $\epsilon_i$  retains the unique contribution of  $x_i$  and removes redundancy.

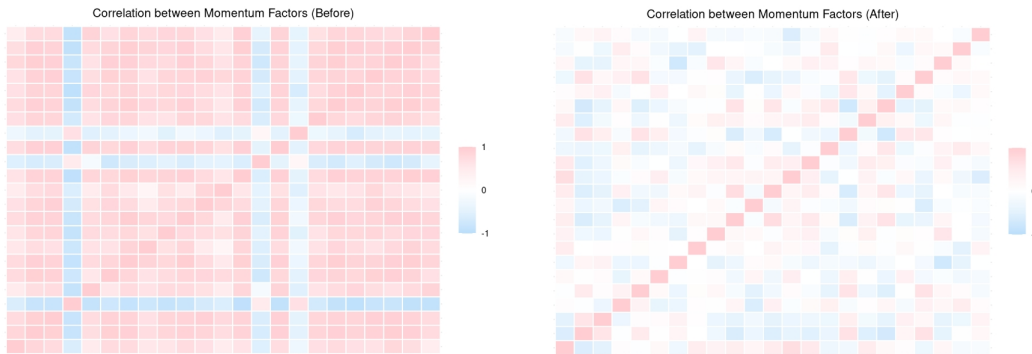


Figure 12: Correlation heatmap of momentum factors before and after de-correlation

Then we also combine the processed factors in each category into a single composite factor by using Principal Component Analysis and taking the first principal component, which represents the majority of information within each category. Then we calculate the correlation matrix between the composite factors to represent the correlation between different categories. As shown in Figure 13, the inter-categorical correlation remains low



before and after de-correlation within each category. This indicates that our grouping method accurately represents different types of factors that may independently affect the financial market.

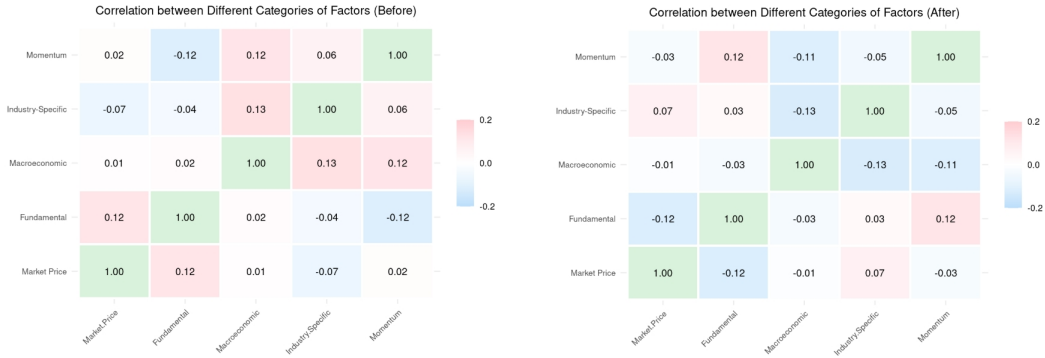


Figure 13: Correlation heatmap between different categories of factors before and after de-correlation within each category

### 4.3 Feature Selection and Prediction Results

After decorrelation of our factors, we train an LSTM model with all factors and an LSTM model with factors selected by CatNet for each stock. We run our algorithm on 100 S&P 500 component stocks. To evaluate whether CatNet can capture the macroeconomic factors that may abnormally influence the market, we set our training set end by 2019-12-31 and evaluate whether our model can predict the unexpected market fluctuations in 2020 during the COVID-19 pandemic. The result shows that the selected macroeconomic factors can effectively estimate the dramatic fluctuation in 2020 in most stocks, and it fits especially well during March 2020, where the stock market plummeted under the pandemic. The LSTM model with selected features also generally performs better in prediction accuracy measured by MSE.

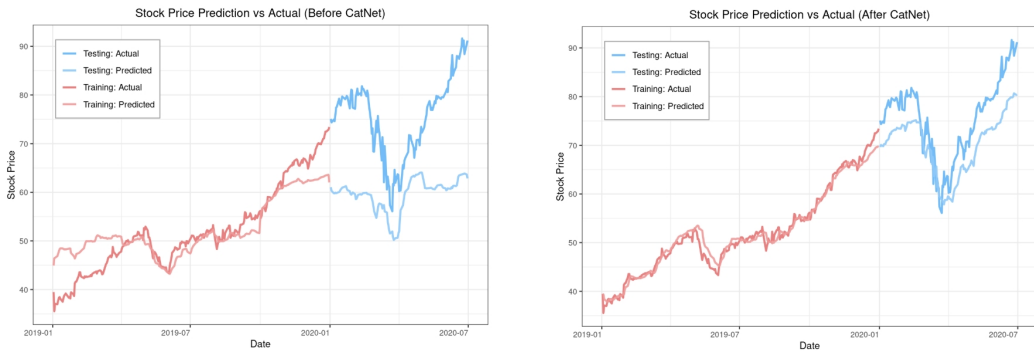


Figure 14: Example of stock prediction before and after CatNet Feature Selection

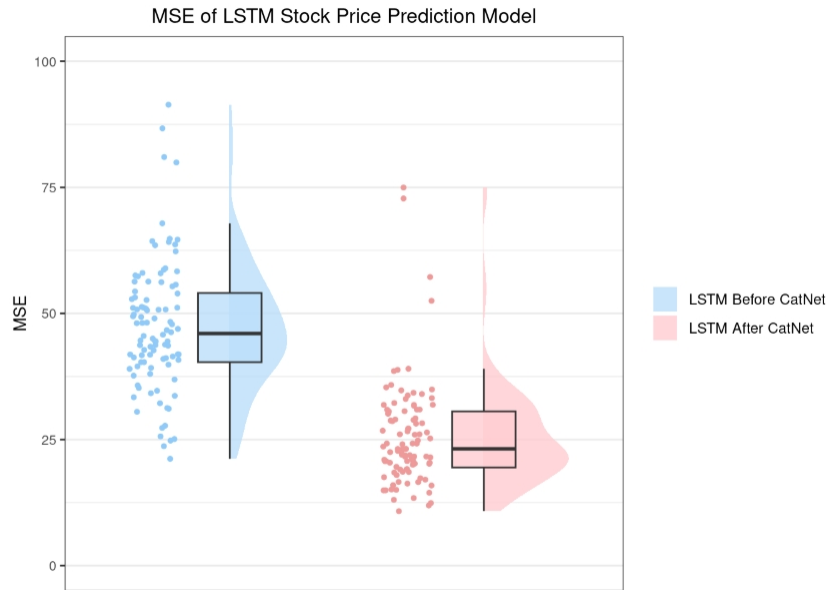


Figure 15: MSE of LSTM stock prediction model before and after CatNet

#### 4.4 Market Interpretation of Selected Factors

After running the algorithm on 100 stocks, we subtract 20 factors which are selected more than 80 times to examine whether these factors effectively reflects general market fluctuations.

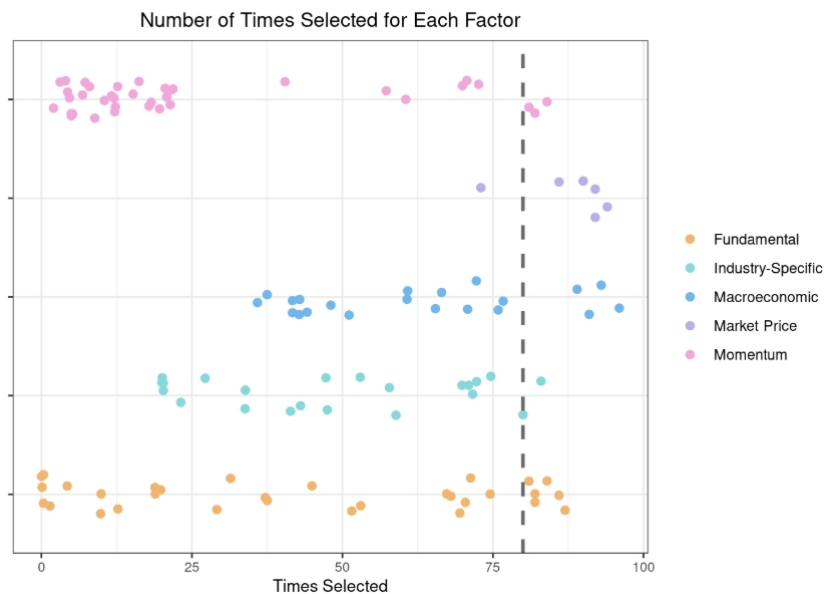


Figure 16: Plot of number of times selected for each stock by categories

Below are examples of these factors and their corresponding financial interpretations:

**Earnings Per Share Basic (EPS):** It is a critical measure of a company's profitability, representing the net profit attributable to each share of stock. Higher EPS often indicates strong profitability and higher expected shareholder returns, acting as a major driver of stock valuation and investor confidence.

**ROE (Return on Equity):** ROE measures a company's ability to generate profit using shareholders' equity, which is a vital indicator of value creation for shareholders. High ROE reflects efficient resource allocation and is often prioritized in investment portfolios. Sustained growth in ROE attracts more capital inflows and drives stock price appreciation.

**CPI (Consumer Price Index):** CPI reflects inflation levels and serves as a significant macroeconomic indicator. High inflation often prompts central banks to tighten monetary policy, increasing financing costs and putting pressure on stock markets. Conversely, low inflation may signal economic weakness. Inflation has a pronounced impact on monetary policy and interest rate adjustments, influencing market dynamics.

**20-Day Price Range:** This factor measures the price fluctuation range over the past 20 days, capturing market volatility and investor sentiment. A wider range often indicates unstable market sentiment, while a narrower range may signal the emergence of a trending market. Price range is also correlated with the volatility index (VIX) and serves as a vital input for momentum trading strategies.

**Finance\_PPI (Finance Industry Producer Price Index):** Finance PPI measures the pricing trends in the financial sector. High PPI indicates strong demand in the financial industry, while low PPI may reflect sluggish activity or rising cost pressures. Changes in financial sector PPI are often directly linked to liquidity conditions and monetary policy adjustments in the capital markets.

Based on our analysis, we find that our algorithm can effectively select the significant factors that generally affect the financial market and make reasonable stock market predictions. This indicates that CatNet, as well as other FDR control methods, has practical applications in improving the interpretability of real-world future predictions.

## 5 Discussions

Our paper introduces a new algorithm, CatNet, for effective feature selection and FDR control in LSTM models. To mitigate the effect of multicollinearity in constructing the mirror variables, we extended the kernel-based dependence measure into time-series and use the weighted average of time-series kernels as the final dependence measure. However, we didn't find an explicit formula for choosing the weights. During the simulation studies, we found that sometimes the mirror statistic for the relevant features still takes a large negative value, indicating that the weights in the model are still unstable due to unexpected high correlations. In later studies, we can try to find a method to guide us choosing the weights by analyzing the structures of LSTMs.

Another clear improvement we can take later is to use the Debiased LASSO [44] instead of normal LASSO for feature pre-selection in linear models with  $p > n$ . In our simulation studies, the mirror statistic for null features appear clearly left-skewed under high-dimensional cases after LASSO, indicating the the LASSO estimator introduces bias into our mirror statistic and thus the estimate for FDR. Using the Debiased LASSO can reduce such bias and maintain the accuracy of our estimate for FDR.

However, despite minor drawbacks that require improvement, our method introduces a new path for constructing the mirror statistic for FDR control. The SHAP value has been widely proven to be generalizable in different Neural Network models and provides a general framework for solving such FDR Control problems in complex models. SHAP values combined with our feature importance vector and time-series kernel dependence, provides a new framework for all time-series prediction models and similar models that require observing the connection between past values and current values, for example, models with Attention mechanisms. In later studies, we can try to extend our methods into these models to examine the generalization property of this method.

## References

- [1] Ahn, T., Lin, L., & Mei, S. (2023). Near-optimal multiple testing in Bayesian linear models with finite-sample FDR control. *arXiv preprint arXiv:2211.02778*. <https://doi.org/10.48550/arXiv.2211.02778>
- [2] Barber, R. F., & Candès, E. J. (2015). Controlling the false discovery rate via knockoffs. *The Annals of Statistics*, 43(5), 2055–2085. <https://doi.org/10.xxxx/yyyy>
- [3] Barber, R. F., & Candès, E. J., et al. (2019). A knockoff filter for high-dimensional selective inference. *The Annals of Statistics*, 47(5), 2504–2537. <https://doi.org/10.xxxx/yyyy>
- [4] Bates, S., Candès, E., Janson, L., & Wang, W. (2021). Metropolized knockoff sampling. *Journal of the American Statistical Association*, 116(535), 1413–1427. <https://doi.org/10.1080/01621459.2020.1729163>
- [5] Benjamini, Y., & Hochberg, Y. (1995). Controlling the false discovery rate: A practical and powerful approach to multiple testing. *Journal of the Royal Statistical Society: Series B (Methodological)*, 57(1), 289–300. <https://www.jstor.org/stable/2346101>
- [6] Berline, A., & Thomas-Agnan, C. (2011). *Reproducing kernel Hilbert spaces in probability and statistics*. Springer Science & Business Media.
- [7] Bühlmann, P., & van de Geer, S. (2011). *Statistics for high-dimensional data: Methods, theory and applications*. Springer. <https://doi.org/10.1007/978-3-642-20192-9>
- [8] Candès, E., Fan, Y., Janson, L., & Lv, J. (2018). Panning for gold: ‘Model-X’ knockoffs for high-dimensional controlled variable selection. *Journal of the Royal Statistical Society: Series B (Statistical Methodology)*, 80(3), 551–577. <https://doi.org/10.xxxx/yyyy>
- [9] Chen, K., Zhou, Y., & Dai, F. (2015). A LSTM-based method for stock returns prediction: A case study of China stock market. In *2015 IEEE International Conference on Big Data (Big Data)* (pp. 2823–2824). IEEE. <https://doi.org/10.1109/BigData.2015.7364089>
- [10] Dai, C. (2020). Methods on model selection: Bayes factor approximation and false discovery rate control [Doctoral dissertation, Harvard University].
- [11] Dai, C., Lin, B., Xing, X., & Liu, J.S. (2020). A Scale-Free Approach for False Discovery Rate Control in Generalized Linear Models. *Journal of the American Statistical Association*, 118, 1551 - 1565.
- [12] Dai, C., Lin, B., Xing, X., & Liu, J. S. (2022). False discovery rate control via data splitting. *Journal of the American Statistical Association*, 118(544), 2503–2520. <https://doi.org/10.1080/01621459.2022.2060113>
- [13] Dai, C., Lin, B., Xing, X., & Liu, J. S. (2023). A scale-free approach for false discovery rate control in generalized linear models. *Journal of the American Statistical Association*, 118(543), 1551–1565. <https://doi.org/10.1080/01621459.2023.2165930>

- [14] Elhoseiny, M., & Elgammal, A. (2015). Generalized twin Gaussian processes using Sharma-Mittal divergence. *arXiv preprint arXiv:1409.7480*. <https://doi.org/10.48550/arXiv.1409.7480>
- [15] Genovese, C. R. (2015). False discovery rate control. In *International Encyclopedia of the Social & Behavioral Sciences* (2nd ed., pp. 242–248). Elsevier. <https://doi.org/10.1016/B978-0-08-097086-8.42001-0>
- [16] Ghorbani, A., Abid, A., & Zou, J. (2019). Interpretation of neural networks is fragile. In *Proceedings of the AAAI Conference on Artificial Intelligence* (pp. 3681–3688).
- [17] Gretton, A., Bousquet, O., Smola, A., & Schölkopf, B. (2005). Measuring statistical dependence with Hilbert-Schmidt norms. In *International Conference on Algorithmic Learning Theory* (pp. 63–77).
- [18] Gretton, A., Bousquet, O., Smola, A., & Schölkopf, B. (2007). A kernel statistical test of independence. In *Neural Information Processing Systems*.
- [19] Hechtlinger, Y. (2016). Interpretation of prediction models using the input gradient. *ArXiv, abs/1611.07634*. <https://arxiv.org/abs/1611.07634>
- [20] Hochreiter, S., & Schmidhuber, J. (1997). Long short-term memory. *Neural Computation*, 9, 1735–1780. <https://doi.org/10.1162/neco.1997.9.8.1735>
- [21] Hothorn, T., Kneib, T., & Bühlmann, P. (2014). Conditional Transformation Models. *Journal of the Royal Statistical Society, Series B (Methodology)*. <https://doi.org/10.1111/rssb.12017>
- [22] Javanmard, A., & Montanari, A. (2018). Debiasing the lasso: Optimal sample size for Gaussian designs. *The Annals of Statistics*, 46(6A), 2593–2622. <https://doi.org/10.1214/17-AOS1630>
- [23] Ke, Z. T., Barber, R. F., & Candès, E. J. (2020). Power of knockoff: The impact of ranking algorithm, augmented design, and symmetric statistic. *Journal of Machine Learning Research*, 25(3), 1–67.
- [24] Le, T.-P., & Argoul, P. (2004). Continuous wavelet transform for modal identification using free decay response. *Journal of Sound and Vibration*, 277(1-2), 73–100. <https://doi.org/10.1016/j.jsv.2003.08.049>
- [25] Liu, S., Zhang, L., & Feng, Q. (2017). CNN-LSTM neural network model for quantitative strategy analysis in stock markets. In *International Conference on Neural Information Processing* (pp. 198–207).
- [26] Lu, Y., Fan, Y., Lv, J., & Noble, W. S. (2018). Deeppink: Reproducible feature selection in deep neural networks. In *Advances in Neural Information Processing Systems* (pp. 8676–8686).

- [27] Luo, D., Ebadi, A., Emery, K., He, Y., Noble, W. S., & Keich, U. (2023). Competition-based control of the false discovery proportion. *Biometrics*, 79(4), 3472–3484. <https://doi.org/10.1111/biom.13830>
- [28] Lundberg, S. M., & Lee, S.-I. (2017). A unified approach to interpreting model predictions. In *Proceedings of the 31st International Conference on Neural Information Processing Systems (NIPS'17)* (pp. 4768–4777). Curran Associates Inc.
- [29] Machkour, J., Palomar, D. P., & Muma, M. (2024). FDR-controlled portfolio optimization for sparse financial index tracking. *ArXiv Preprint*, arXiv:2401.15139. <https://arxiv.org/abs/2401.15139>
- [30] Messai, A., Drif, A., Ouyahia, A., Guechi, M., Rais, M., & Kaderali, L. (2024). Towards XAI agnostic explainability to assess differential diagnosis for meningitis diseases. *Machine Learning: Science and Technology*. <https://doi.org/10.1088/2632-2153/ad4a1f>
- [31] Mooij, J.M., Janzing, D., Peters, J., & Schölkopf, B. (2009). Regression by dependence minimization and its application to causal inference in additive noise models. *International Conference on Machine Learning*.
- [32] Muandet, K., Fukumizu, K., Sriperumbudur, B., & Schölkopf, B. (2017). Kernel mean embedding of distributions: A review and beyond. *Foundations and Trends in Machine Learning*, 10(1–2), 1–141. <https://doi.org/10.1561/22000000060>
- [33] Nelson, D. M. Q., Pereira, A. C. M., & de Oliveira, R. A. (2017). Stock market's price movement prediction with LSTM neural networks. In *2017 International Joint Conference on Neural Networks (IJCNN)* (pp. 1419–1426). IEEE. <https://doi.org/10.1109/IJCNN.2017.7966019>
- [34] Pascanu, R., Mikolov, T., & Bengio, Y. (2013). On the difficulty of training recurrent neural networks. In *Proceedings of the 30th International Conference on Machine Learning (ICML'13)* (pp. III–1310–III–1318).
- [35] Sherstinsky, A. (2018). Fundamentals of recurrent neural network (RNN) and long short-term memory (LSTM) network. *ArXiv Preprint*, arXiv:1808.03314. <https://arxiv.org/abs/1808.03314>
- [36] Shi, Y., Wang, Y., Qu, Y., & Chen, Z. (2023). Integrated GCN-LSTM stock prices movement prediction based on knowledge-incorporated graphs construction. *International Journal of Machine Learning and Cybernetics*, 15, 161–176. <https://doi.org/10.1007/s13042-023-01817-6>
- [37] Tibshirani, R. (1996). Regression shrinkage and selection via the lasso. *Journal of the Royal Statistical Society: Series B (Methodological)*, 58(1), 267–288. <https://www.jstor.org/stable/2346178>
- [38] Verikas, A., & Bacauskiene, M. (2002). Feature selection with neural networks. *Pattern Recognition Letters*, 23(11), 1323–1335.

- [39] Wang, T., & Li, W. (2017). Kernel learning and optimization with Hilbert–Schmidt independence criterion. *International Journal of Machine Learning and Cybernetics*, 9, 1707 - 1717.
- [40] Woodward, W. A., Gray, H. L., & Elliott, A. C. (2014). Applied Time Series Analysis. *International Statistical Review*, 82(2). <https://doi.org/10.1111/insr.12068>.11
- [41] Xing, X., Zhao, Z., & Liu, J. S. (2020). Neural Gaussian mirrors for controlling false discovery rate in deep learning models. *ArXiv Preprint*, *arXiv:2010.06175v1*. <https://arxiv.org/abs/2010.06175>
- [42] Xing, X., Zhao, Z., & Liu, J. S. (2021). Controlling false discovery rate using Gaussian mirrors. *ArXiv Preprint*, *arXiv:1911.09761v3*. <https://arxiv.org/abs/1911.09761>
- [43] Y, F.-J., & Li, L. (2010). Integrable coupling system of JM equations hierarchy with self-consistent sources. *Communications in Theoretical Physics*, 54(3), 385–390. <https://doi.org/10.1088/0253-6102/54/3/19>
- [44] Zhang, C., & Zhang, S. (2011). Confidence intervals for low dimensional parameters in high dimensional linear models. *Journal of the Royal Statistical Society: Series B (Statistical Methodology)*, 76.
- [45] Zhu, Z., Fuhrman, J. A., Sun, F., & Noble, W. S. (2021). DeepLINK: Deep learning inference using knockoffs with applications to genomics. *Proceedings of the National Academy of Sciences of the United States of America*, 118(36), e2104683118. <https://doi.org/10.1073/pnas.2104683118>
- [46] Zuo, W., Zhu, Z., Du, Y., Yeh, Y.-C., Fuhrman, J. A., Lv, J., Fan, Y., & Sun, F. (2024). DeepLINK-T: Deep learning inference for time series data using knockoffs and LSTM.



## Appendix

### A. Important Properties of SHAP

SHAP Values satisfy the following important properties:

**Lemma 1 (Efficiency):** The sum of feature contributions equals the difference between the prediction for  $x$  (the predicted value of  $y$ ) and the expected prediction.

$$\sum_{j=1}^p \Phi_j = \hat{f}(x) - \mathbb{E}_X[\hat{f}(X)]$$

**Lemma 2 (Symmetry):** If two features  $j$  and  $k$  contribute equally to all possible coalitions, then their SHAP values should be the same.

if  $\text{val}(S \cup \{x_j\}) = \text{val}(S \cup \{x_k\})$  for all  $S \subseteq \{x_1, \dots, x_p\} \setminus \{x_j, x_k\}$ , then  $\Phi_j = \Phi_k$

**Lemma 3 (Additivity):** For games with combined payoffs, the corresponding SHAP value is given by the sum of the SHAP values from the individual games.

$$\Phi_j^{v_1+v_2} = \Phi_j^{v_1} + \Phi_j^{v_2}$$

Besides the three basic properties above, we can get the following important properties of SHAP values that allows us to construct the feature importance metric:

**Property 1:** The value function for an empty set  $\emptyset$  is zero.

$$v(\emptyset) = \int f(\mathbf{X}_1, \dots, \mathbf{X}_p) dP(\mathbf{X}) - \mathbb{E}[f(\mathbf{X})] = \mathbb{E}[f(\mathbf{X})] - \mathbb{E}[f(\mathbf{X})] = 0$$

**Property 2:** For a null feature  $j$ , its SHAP value should have expectation zero.

By definition,  $j$  does not change the prediction regardless of which coalition it is added to and what its value, so we have:

$$v(S \cup \{j\}) - v(S) = 0, \quad \text{for all } S \subseteq \{1, \dots, p\} \setminus \{j\}.$$

Thus, the expected SHAP value is given by:

$$\mathbb{E}[\Phi_j^i] = \sum_{S \subseteq \{1, \dots, p\} \setminus \{j\}} \frac{|S|!(p - |S| - 1)!}{p!} \cdot \mathbb{E}[v(S \cup \{j\}) - v(S)] = \sum_{S \subseteq \{1, \dots, p\} \setminus \{j\}} 0 = 0.$$

**Property 3:** Under some assumption, for a null feature  $j$ , the estimated SHAP value using Monte-Carlo integration should be asymptotically symmetric.

Due to model fitting errors and data noise, the model output may exhibit a slight dependence on  $x_j$  even if feature  $j$  is a null feature. We consider this dependence, along with the randomness introduced by Monte Carlo sampling, as random error:

$$\epsilon_{S_j}^{(k)} = f\left(x_{S \cup \{j\}}^{(i)} \cup X_{C \setminus \{j\}}^{(k)}\right) - f\left(x_S^{(i)} \cup X_C^{(k)}\right).$$

These errors,  $\epsilon_{S_j}^{(k)}$ , are random variables reflecting the estimation error for null feature  $j$ .

In the case where feature  $j$  is a null feature, we have:

$$\mathbb{E}[\hat{\Phi}_j^i] = \sum_S \omega(S) \mathbb{E}[\Delta_{S_j}] = \sum_S \omega(S) \left(\frac{1}{n} \sum_{k=1}^n \mathbb{E}[\epsilon_{S_j}^{(k)}]\right) = 0.$$

The variance of the estimated marginal contribution is:

$$\text{Var}[\Delta_{S_j}] = \text{Var}\left[\frac{1}{n} \sum_{k=1}^n \epsilon_{S_j}^{(k)}\right] = \frac{1}{n^2} \sum_{k=1}^n \text{Var}[\epsilon_{S_j}^{(k)}] = \frac{\sigma_{S_j}^2}{n},$$

where  $\sigma_{S_j}^2 = \text{Var}[\epsilon_{S_j}(k)]$ .

The variance of the estimated SHAP value is:

$$\text{Var}[\hat{\Phi}_j^i] = \text{Var}\left[\sum_S \omega(S) \Delta_{S_j}\right] = \sum_S \omega(S)^2 \text{Var}[\Delta_{S_j}] = \sum_S \frac{\omega(S)^2 \sigma_{S_j}^2}{n}.$$

Since  $\hat{\Phi}_j^i$  is a linear combination of multiple independent random variables, according to the Central Limit Theorem (CLT), the distribution of  $\hat{\Phi}_j^i$  will converge to a normal distribution as  $n \rightarrow \infty$ . Specifically, the distribution of  $\hat{\Phi}_j^i$  can be approximated by:

$$\hat{\Phi}_j^i \sim N\left(0, \frac{1}{n} \sum_S \omega(S)^2 \sigma_{S_j}^2\right),$$

which is asymptotic symmetric, as long as the following conditions hold:

1. For fixed  $S$  and  $j$ ,  $\epsilon_{S_j}^{(k)}$  are i.i.d. random variables.
2.  $\text{Var}[\epsilon_{S_j}^{(k)}]$  is finite.

## B. Expectation of SHAP Feature Importance Metric in Linear Regression

The SHAP value for a feature  $x_i$  is defined as:

$$\Phi_i = \sum_{S \subseteq N \setminus \{i\}} \frac{|S|!(n - |S| - 1)!}{n!} [f(S \cup \{i\}) - f(S)]$$

Consider a linear regression model:

$$y = f(x) = \beta_0 + \beta_1 x_1 + \beta_2 x_2 + \cdots + \beta_p x_p + \epsilon$$

The OLS estimation equation of the model should be:

$$\hat{y} = \hat{\beta}_0 + \hat{\beta}_1 x_1 + \hat{\beta}_2 x_2 + \cdots + \hat{\beta}_p x_p, \quad \text{where } E(\hat{\beta}_j) = \beta_j$$

For the feature  $j$ , its marginal contribution is defined as:

$$\Delta f_j = f(S \cup \{j\}) - f(S)$$

In a linear regression model, features not included in the subset  $S$  are replaced with their expected values. So when the feature  $j$  is included:

$$f(S \cup \{j\}) = \hat{\beta}_0 + \sum_{i \in S} \hat{\beta}_i x_i + \hat{\beta}_j x_j + \sum_{k \notin S \cup \{j\}} \hat{\beta}_k E(x_k)$$

When the feature  $x_j$  is not included:

$$f(S) = \hat{\beta}_0 + \sum_{i \in S} \hat{\beta}_i x_i + \sum_{k \notin S \cup \{j\}} \hat{\beta}_k E(x_k) + \hat{\beta}_j E(x_j)$$

Thus, the marginal contribution of feature  $x_j$  is:

$$\Delta f_j = \hat{\beta}_j x_j - \hat{\beta}_j E(x_j) = \hat{\beta}_j (x_j - E(x_j))$$

Due to the linearity and additivity of the model, the SHAP value for  $x_j$  simplifies to:

$$\Phi_j = \hat{\beta}_j (x_j - E(x_j))$$

However, we calculate the SHAP value for  $x_j$  using Monte Carlo Integration, so the estimated value should have some error. Based on the unbiasedness of Monte Carlo Estimation, we write it as:

$$\hat{\Phi}_j = \hat{\beta}_j (x_j - E(x_j)) + \epsilon_j, \quad \text{where } E(\epsilon_j) = 0$$

Now, we use simple linear regression to fit the SHAP values based on the dataset  $(x_j^i, \hat{\Phi}_j^i)$ . The estimation equation should be:

$$\tilde{\Phi}_j = \tilde{\beta}_0 + \tilde{\beta}_j x_j$$

Taking the derivative of the fitted function, we have

$$\tilde{\phi}_j = \frac{\partial \tilde{\Phi}_j}{\partial x_j} = \tilde{\beta}_j$$

Since  $E(\epsilon_j) = 0$ , by the property of the OLS estimator, we conclude that:

$$E(\tilde{\phi}_j) = E(\tilde{\beta}_j) = E(E(\tilde{\beta}_j)) = E(\hat{\beta}_j) = \beta_j$$

### C. HSIC Value for Linear Kernel

In this section, we show that when using a linear kernel and ignoring time-series correlations, the HSIC value is proportional to the square of the Pearson correlation coefficient.

Given two variables  $X$  and  $Y$  with  $n$  samples  $\{(x_i, y_i)\}_{i=1}^n$ , we define HSIC (Hilbert-Schmidt Independence Criterion):

$$\text{HSIC}_n(X, Y) = \frac{1}{n^2} \text{tr}(\tilde{K}\tilde{L}),$$

where  $\tilde{K}$  and  $\tilde{L}$  are the centered kernel matrices for  $X$  and  $Y$ .

For simplicity, we assume that both  $X$  and  $Y$  are centered, i.e.,  $\sum_{i=1}^n x_i = 0$  and  $\sum_{i=1}^n y_i = 0$ .

When using the linear kernel  $k(x_i, x_j) = x_i x_j$ , the kernel matrices  $K$  for  $X$  and  $Y$  are:

$$K_{ij} = x_i x_j \quad L_{ij} = y_i y_j$$

Since  $X$  and  $Y$  are already centered, the kernel matrices  $K$  and  $L$  are automatically centered:

$$\tilde{K} = K, \quad \tilde{L} = L.$$

So the HSIC value is

$$\text{HSIC}_n(X, Y) = \frac{1}{n^2} \text{tr}(\tilde{K}\tilde{L}) = \frac{1}{n^2} \text{tr}(KL).$$

Expanding  $\text{tr}(KL)$ , substituting  $K_{ij} = x_i x_j$  and  $L_{ji} = y_j y_i$ , we get:

$$\text{tr}(KL) = \sum_{i=1}^n \sum_{j=1}^n K_{ij} L_{ji} = \sum_{i=1}^n \sum_{j=1}^n x_i x_j y_j y_i = \left( \sum_{i=1}^n x_i y_i \right)^2.$$

So the HSIC value becomes:

$$\text{HSIC}_n(X, Y) = \frac{1}{n^2} \left( \sum_{i=1}^n x_i y_i \right)^2.$$

We know the Pearson correlation coefficient is:

$$\rho(X, Y) = \frac{\text{Cov}(X, Y)}{\sigma_X \sigma_Y} = \frac{\frac{1}{n} \sum_{i=1}^n x_i y_i}{\sqrt{\frac{1}{n} \sum_{i=1}^n x_i^2} \sqrt{\frac{1}{n} \sum_{i=1}^n y_i^2}}.$$

Let  $S_{XY} = \sum_{i=1}^n x_i y_i$ ,  $S_X = \sum_{i=1}^n x_i^2$ , and  $S_Y = \sum_{i=1}^n y_i^2$ . Then:

$$\text{HSIC}_n(X, Y) = \frac{1}{n^2} S_{XY}^2, \quad \rho(X, Y) = \frac{\frac{1}{n} S_{XY}}{\sqrt{\frac{1}{n} S_X} \sqrt{\frac{1}{n} S_Y}} = \frac{S_{XY}}{\sqrt{S_X S_Y}}.$$

Squaring  $\rho(X, Y)$ :

$$\rho(X, Y)^2 = \frac{S_{XY}^2}{S_X S_Y}.$$

Substituting  $S_{XY}^2$  into the HSIC expression:

$$\text{HSIC}_n(X, Y) = \frac{1}{n^2} S_{XY}^2 = \frac{1}{n^2} \rho(X, Y)^2 S_X S_Y.$$

So we have shown that the HSIC value is proportional to the square of the Pearson correlation coefficient, and the proportion depends on the sample size  $n$  and the variances of  $X$  and  $Y$ .